

Conditional Knockout of the Menkes Disease Copper Transporter Demonstrates Its Critical Role in Embryogenesis

Yanfang Wang^{1,2,3}, Sha Zhu^{1,3}, Gary A. Weisman^{1,3}, Jonathan D. Gitlin⁴, Michael J. Petris^{1,2,3*}

1 Department of Biochemistry, University of Missouri, Columbia, Missouri, United States of America, **2** Department of Nutrition and Exercise Physiology, University of Missouri, Columbia, Missouri, United States of America, **3** The Christopher S. Bond Life Science Center, University of Missouri, Columbia, Missouri, United States of America, **4** Marine Biological Laboratory, Woods Hole, Massachusetts, United States of America

Abstract

The transition metal, copper (Cu), is an enzymatic cofactor required for a wide range of biochemical processes. Its essentiality is demonstrated by Menkes disease, an X-linked copper deficiency disorder characterized by defects in nervous-, cardiovascular- and skeletal systems, and is caused by mutations in the ATP7A copper transporter. Certain ATP7A mutations also cause X-linked Spinal Muscular Atrophy type 3 (SMAX3), which is characterized by neuromuscular defects absent an underlying systemic copper deficiency. While an understanding of these ATP7A-related disorders would clearly benefit from an animal model that permits tissue-specific deletion of the ATP7A gene, no such model currently exists. In this study, we generated a floxed mouse model allowing the conditional deletion of the *Atp7a* gene using Cre recombinase. Global deletion of *Atp7a* resulted in morphological and vascular defects in hemizygous male embryos and death *in utero*. Heterozygous deletion in females resulted in a 50% reduction in live births and a high postnatal lethality. These studies demonstrate the essential role of the *Atp7a* gene in mouse embryonic development and establish a powerful model for understanding the tissue-specific roles of ATP7A in copper metabolism and disease.

Citation: Wang Y, Zhu S, Weisman GA, Gitlin JD, Petris MJ (2012) Conditional Knockout of the Menkes Disease Copper Transporter Demonstrates Its Critical Role in Embryogenesis. PLoS ONE 7(8): e43039. doi:10.1371/journal.pone.0043039

Editor: Steven R. Ellis, University of Louisville, United States of America

Received: June 1, 2012; **Accepted:** July 16, 2012; **Published:** August 10, 2012

Copyright: © 2012 Wang et al. This is an open-access article distributed under the terms of the Creative Commons Attribution License, which permits unrestricted use, distribution, and reproduction in any medium, provided the original author and source are credited.

Funding: This work was supported by National Institutes of Health Grants DK59893 and DK093386 to M.J.P., and DK44464 to J.D.G. The funders had no role in study design, data collection and analysis, decision to publish, or preparation of the manuscript.

Competing Interests: The authors have declared that no competing interests exist.

* E-mail: petrism@missouri.edu

These authors contributed equally to this work.

Introduction

The ability of copper to cycle between Cu¹⁺ and Cu²⁺ oxidation states enables it to function as a cofactor within a host of enzymes that catalyze a wide range of biochemical reactions. These include cellular respiration (cytochrome oxidase), connective tissue formation (lysyl oxidase), catecholamine synthesis (dopamine β hydroxylase), pigmentation (tyrosinase) and neuropeptide processing (peptidylglycine α-amidating monooxygenase) [1]. Not surprisingly, copper deficiency during gestation results in pleiotropic defects ranging from early embryonic lethality to long term postnatal defects in nervous-, circulatory- and skeletal systems [2]. The consequences of copper deficiency in humans are illustrated by Menkes disease (OMIM 390400), a pediatric disorder of copper metabolism caused by mutations in the ATP7A gene (NM_000052). The affected protein, ATP7A, is a copper transporting P-type ATPase that is predominantly located in the distal compartments of the Golgi complex where it loads copper into the secretory pathway for incorporation into nascent polypeptides [3,4]. The ATP7A protein also functions in cellular copper export, which is coupled to copper-stimulated trafficking of the protein into post-Golgi vesicles that fuse with the plasma membrane [3].

Menkes disease patients exhibit a wide spectrum of defects that are attributable to copper deficiency, including connective tissue malformation giving rise to hemorrhage, neurological symptoms such as mental retardation and seizures, and hypopigmentation due to defects in melanin synthesis [1]. Occipital horn syndrome (OMIM 304150) is another variant of this disorder in which connective tissue defects predominate with little or no neurological abnormality [5]. As an X-linked recessive trait, Menkes patients are typically male, although heterozygous female carriers may exhibit subtle phenotypes such as mosaic hypopigmentation due to variation in X-chromosome inactivation [6]. Recently, two missense mutations in the ATP7A gene were shown to cause X-linked distal spinal muscular atrophy type 3 (SMAX3; OMIM 300489), a degenerative neuromuscular disorder that typically affects patients in the second or third decade of life. Although *in vitro* studies suggest that SMAX3-causing mutations diminish ATP7A copper transport activity and localization, a systemic copper deficiency is lacking in SMAX3 patients suggesting that the motor neurons may be hypersensitive to subtle perturbations in copper homeostasis [1,7].

The striking differences between Menkes disease, OHS and SMAX3, particularly in the affected organs, highlights the need to understand the functions of ATP7A at a tissue-specific level. However, there is currently no animal model that allows ATP7A

deletion to be restricted to a given tissue. Whereas spontaneous mutations in the *Atp7a* gene have been identified in the collection of Mottled mice, named for the variegated coat color of heterozygous females, these mutants are limited in addressing the tissue-specific functions of the Atp7a protein due in part to the fact that *Atp7a* null mutations are embryonic lethal, as seen in the Dappled and Tohoku mutants, [8–10]. Thus, the only available mutants for study are those in which mutations only partially disrupt Atp7a protein activity (e.g., Brindled or Blotchy mice) [11]. In addition, since the *Atp7a* gene is ubiquitously expressed, certain phenotypes in the Mottled mice may be secondary to defects in copper homeostasis in other tissues. In this study, we describe the generation of an *Atp7a* “floxed” mouse model by homologous integration of Lox P sites into the sequences surrounding exon 11. Global deletion of the *Atp7a* gene in male hemizygotes using Cre recombinase resulted in embryonic lethality and a loss of Atp7a protein expression. These findings provide unequivocal evidence that *Atp7a* is required for embryogenesis and provide a powerful template for elucidating the spatiotemporal requirements for *Atp7a* *in vivo*.

Results

Generation of a Floxed *Atp7a* Mouse Model

A targeting construct encompassing exons 8 to 13 of the *Atp7a* gene was generated with Lox P sites flanking exon 11. Since this exon encodes a region of Atp7a protein that is highly conserved across orthologues of different phyla, its deletion by Cre recombinase was predicted to result in a nonfunctional protein (Figure 1). The targeting construct also contained a neomycin resistance cassette that was driven by the phosphoglycerate kinase 1 promoter and flanked by FLP recombination sites (Figure 1). Recombinant embryonic stem cells with homologous integration of the targeting vector were microinjected into Balb/c blastocysts. The resulting chimeras with a high percentage black coat color were mated to wild-type C57BL6 mice to generate F1 offspring carrying the recombinant *Atp7a* allele. The neomycin cassette was then removed by cross breeding the F1 mice with C57BL6 mice expressing FLP recombinase to generate males and females

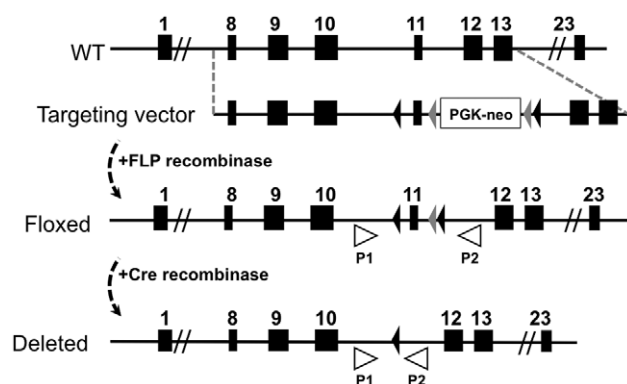


Figure 1. Schematic representation of the *Atp7a* gene-targeting strategy. Exons 8–13 of the wild type and recombinant *Atp7a* locus are shown. The targeting construct included LoxP sites (black triangles) that flanked exon 11 and a PGKneo gene cassette flanked by FRT sites (grey triangles). The PGKneo gene cassette was removed by crossbreeding with the ACT-FLPe deleter strain expressing FLP1 recombinase to generate mice with the desired floxed allele (*Atp7a^{fl/y}*). The exon 11-deleted *Atp7a* allele (Deleted) is depicted following excision by Cre recombinase, which was detected using PCR primers P1 and P2.

doi:10.1371/journal.pone.0043039.g001

harboring the floxed *Atp7a* allele, hereafter designated *Atp7a^{fl}* (Figure 1).

Global knockout of the *Atp7a* gene

To test whether Cre recombinase-mediated excision of exon 11 would generate a null allele of *Atp7a*, we crossed heterozygous floxed females (*Atp7a^{fl/y}*) with mice that express Cre recombinase early in development throughout the epiblast by embryonic day 6.5 (E6.5) driven from the endogenous *Claudin 6* gene promoter (*Cldn6Cre^{+/+}*). An absence of *Atp7a^{fl/y}; Cldn6Cre^{+/-}* hemizygous male pups among a total of 80 live births suggested that this genotype was embryonic lethal (Table 1), and was consistent with our finding of only half the expected ratio of *Atp7a^{fl/y}; Cldn6Cre^{+/-}* heterozygous females among these offspring. Of the 16 *Atp7a^{fl/y}; Cldn6Cre^{+/-}* female pups, only two lived beyond the second day of birth and these survivors exhibited a mosaic pattern of hypopigmented coat coloring (Figure 2A and 2B), which was reminiscent of the variable pattern of X-chromosome inactivation that gives rise to the variegated coat color in heterozygous female carriers of Mottled mutations [12]. These females also exhibited curly whiskers (pili torti) (Figure 2C), a well-documented feature of copper deficiency in the male hemizygous Mottled mutants [13]. Taken together, these results suggest that global excision of exon 11 of the *Atp7a* gene results in embryonic lethality in male hemizygotes, and a partially dominant haploinsufficiency in heterozygous females.

To verify that the absence of Cre-positive floxed males among live births was not due to a failure of conception, embryos were collected and genotyped at E10.5. Of a total of 64 embryos analyzed, 13 were identified as Cre-positive floxed males (*Atp7a^{fl/y}; Cldn6Cre^{+/-}*), which was close to the expected Mendelian ratio of 25% (Table 1). PCR analysis of the yolk sac DNA confirmed highly efficient cleavage of exon 11 in the male hemizygous *Atp7a^{fl/y}; Cldn6Cre^{+/-}* embryos, and the presence of both wild type and cleaved alleles in heterozygous *Atp7a^{fl/y}; Cldn6Cre^{+/-}* embryos (Figure 3A). Immunoblot analysis demonstrated an absence of Atp7a protein in the male hemizygous *Atp7a^{fl/y}; Cldn6Cre^{+/-}* embryos (Figure 3B), and, as expected, the extent of this reduction was variable in *Atp7a^{fl/y}; Cldn6Cre^{+/-}* heterozygous female embryos (Figure 3B). The E10.5 male knockout embryos were smaller than wild type sibling embryos, and exhibited striking morphological defects in the frontonasal region and the orientation of the tail bud (Figure 4A). There was also a notable absence of a blood-filled vascular network in the knockout embryo and the surrounding yolk sac (Figure 4A and 4B). These findings confirmed the essentiality of *Atp7a* in embryonic development and establish a conditional knockout mouse model of this gene.

Characterization of wild type and knockout embryonic fibroblasts

Cell clones in which the presence or absence of a given protein is the sole genetic variable can often provide a powerful *in vitro* model for understanding its cellular function. To develop such a model for ATP7A, wild type mouse embryonic fibroblasts were obtained from E13.5 *Atp7a^{fl/y}* floxed male embryos and then immortalized by transfection of a plasmid encoding the SV40 large T antigen. A single clone, MEF7a⁺, was obtained after neomycin selection in which the Atp7a protein was detected by immunoblotting (Figure 5A). Stable MEF7a⁻ derivatives of this cell line lacking expression of the Atp7a protein were cloned by transient transfection of MEF7a⁺ cells with a plasmid encoding Cre recombinase to excise Exon 11 of the *Atp7a* gene (Figure 5A). Since Atp7a mediates the transport of copper from the cytoplasm into the Golgi, we investigated whether this function was lacking in

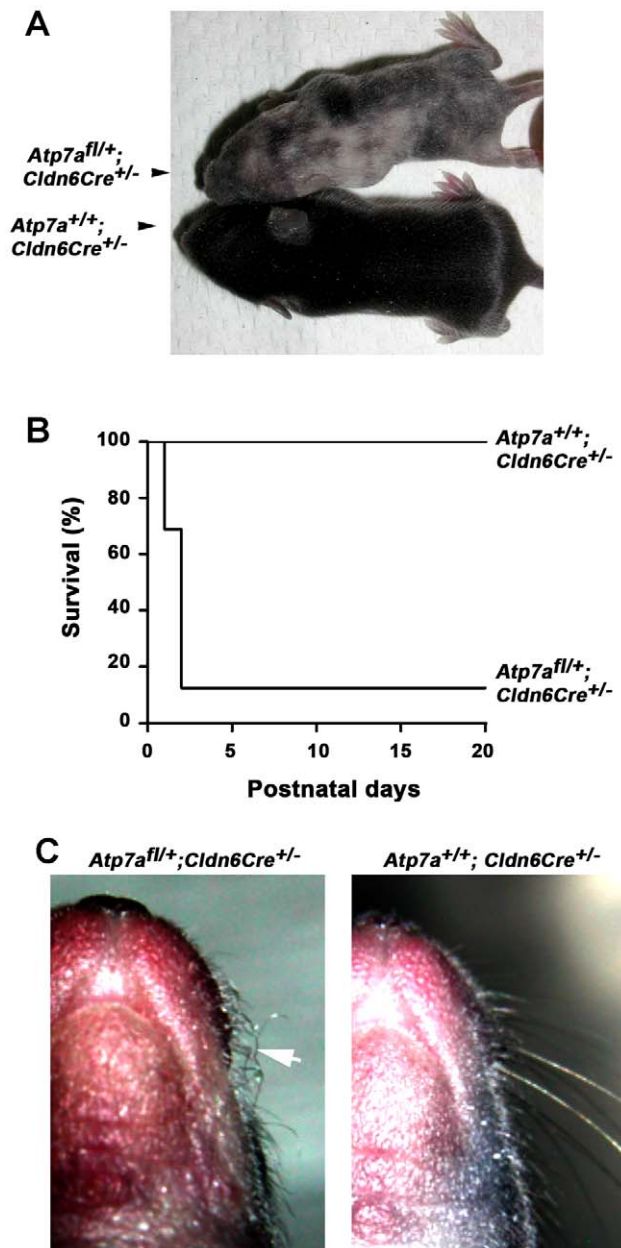


Figure 2. Characterization of *Atp7a*^{fl/+}; *Cldn6Cre*^{+/-} heterozygous female mice. A) Patches of hypopigmentation are observed in the coats of weanling heterozygous *Atp7a*^{fl/+}; *Cldn6Cre*^{+/-} females. B) Kaplan-Meier plot showing postnatal survival of heterozygous *Atp7a*^{fl/+}; *Cldn6Cre*^{+/-} female (n = 16) and littermate control *Atp7a*^{+/+}; *Cldn6Cre*^{+/-} (n = 34). C) Pili torti of the whiskers in surviving *Atp7a*^{fl/+}; *Cldn6Cre*^{+/-} females is shown (arrow).
doi:10.1371/journal.pone.0043039.g002

MEF7a⁻ cells. Transfection of a plasmid encoding tyrosinase, an enzyme that requires copper loading within the secretory pathway via the *Atp7a* protein [14], resulted in the production of the DOPochrome pigment in MEF7a⁺ cells, but not in MEF7a⁻ cells (Figure 5B). The failure to produce DOPochrome in MEF7a⁻ cells was due to a lack of *Atp7a*-mediated copper delivery to tyrosinase because DOPochrome was produced when MEF7a⁻ cells were co-transfected with both tyrosinase and ATP7A expression plasmids (Figure 5B). Additional studies demonstrated that the activity of a copper-inducible luciferase reporter plasmid

Table 1. Frequency of offspring with global deletion of the *Atp7a* gene.

Genotype	Live births	E10.5	Expected
<i>Atp7a</i> ^{+/-} ; <i>Cldn6Cre</i> ^{+/-}	30	17	25%
<i>Atp7a</i> ^{fl/+} ; <i>Cldn6Cre</i> ^{+/-}	0	13	25%
<i>Atp7a</i> ^{fl/+} ; <i>Cldn6Cre</i> ^{+/-}	16	14	25%
<i>Atp7a</i> ^{+/+} ; <i>Cldn6Cre</i> ^{+/-}	34	20	25%
Total	80	64	100%

The numbers of live-born offspring or embryos at day 10.5 post coitus (E10.5) are shown for each genotype resulting from a cross between *Atp7a*^{fl/+} females and *Atp7a*^{+/-}; *Cldn6Cre*^{+/-} males.

doi:10.1371/journal.pone.0043039.t001

was higher following transfection of MEF7a⁻ cells relative to MEF7a⁺ cells, consistent with higher cytoplasmic copper levels resulting from the loss of *Atp7a* protein (Figure 5C). This was further supported by the finding of lower levels of the Ccs protein in MEF7a⁻ cells relative to MEF7a⁺ cells (Figure 5D), a protein whose abundance is inversely proportional to copper concentration [15,16].

Discussion

The striking morphological and vascular defects observed in *Atp7a*^{fl/+}; *Cldn6Cre*^{+/-} embryos at E10.5 resembled the phenotype of the most severe Mottled mutant in which embryonic lethality

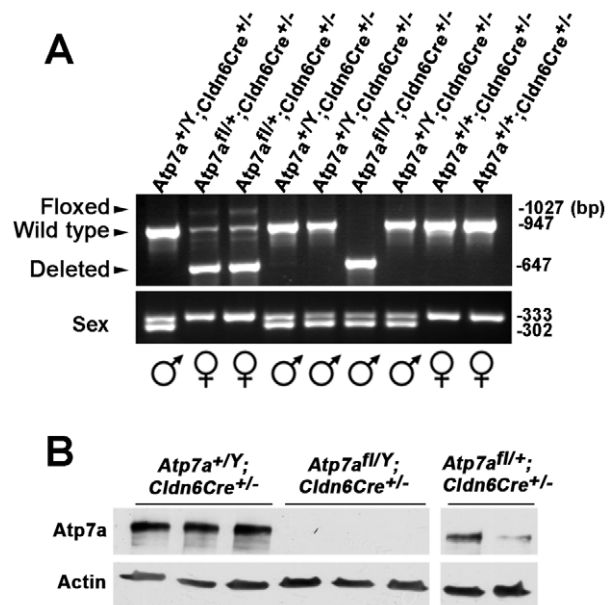


Figure 3. Exon 11 deletion in male hemizygous *Atp7a*^{fl/Y}; *Cldn6Cre*^{+/-} embryos. A) PCR analysis with P1 and P2 primers of yolk sac DNA of E10.5 embryos generated by crossing heterozygous floxed female mice (*Atp7a*^{fl/+}) with *Cldn6Cre* mice (*Atp7a*^{+/-}; *Cldn6Cre*^{+/-}). Cre-mediated deletion of the floxed allele (floxed) was detected by the presence of a 647 bp PCR product (Deleted). Sex was determined by PCR amplification of yolk sac DNA to simultaneously detect the X-chromosome-specific *Jarid1c* gene (331 bp) and the Y-chromosome-specific *Jarid1d* gene (302 bp). B) Immunoblot detection of *Atp7a* protein in E10.5 embryos. Blots were probed with anti-*Atp7a* antibody (1:5000) followed by HRP-conjugated anti-rabbit antibody (1:5000). Actin protein was detected on the same blot as a loading control.
doi:10.1371/journal.pone.0043039.g003

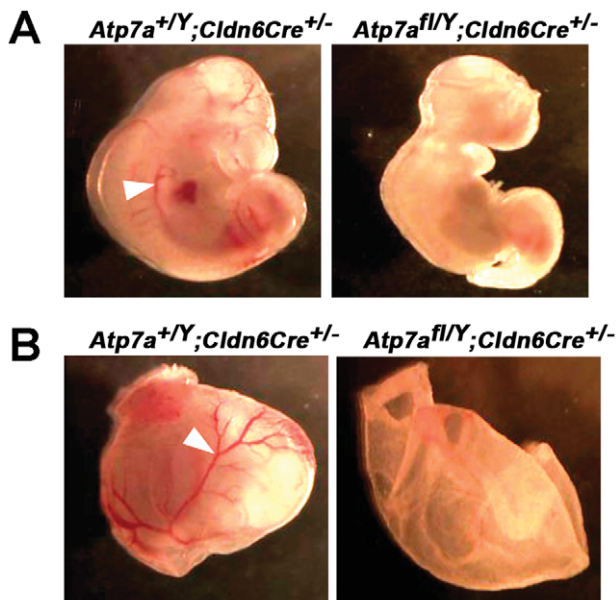


Figure 4. Morphological and vascular abnormalities in male hemizygous *Atp7a*^{fl/Y}; *Cldn6Cre*^{+/-} embryos. A) Developmental anomalies particularly in the frontonasal region and tail bud orientation were apparent in the *Atp7a*^{fl/Y}; *Cldn6Cre*^{+/-} embryos at E10.5. B) The blood-filled vascular network observed in wild type embryos and yolk sacs (arrowheads) was lacking for the *Atp7a*^{fl/Y}; *Cldn6Cre*^{+/-}. doi:10.1371/journal.pone.0043039.g004

occurs at a similar stage of gestation [10]. Thus, the results presented in this study provide conclusive evidence that global deletion of the *Atp7a* gene in mice results in embryonic lethality. Although the precise biochemical basis for embryonic lethality in mice lacking an intact *Atp7a* gene is unknown, the *Atp7a* protein is known to deliver copper to at least three copper-containing enzymes whose deletion has been shown to cause lethality during gestation or the perinatal period, including peptidyl-glycine alpha-amidating monooxygenase, dopamine beta hydroxylase and lysyl oxidase [17–19]. Thus, it is reasonable to conclude that the phenotype of *Atp7a*^{fl/Y}; *Cldn6Cre*^{+/-} embryos is likely to stem from hypoactivity of these enzymes, and possibly others that acquire copper via the secretory pathway. It was also interesting to note that while heterozygous deletion of *Atp7a* in our study generated a high rate of postnatal mortality, heterozygous Mottled females are viable and able to propagate even the embryonic lethal Mottled mutations [11]. We speculate that the more severe phenotype in our heterozygous females may be due to the C57BL6 mouse background on which *Atp7a* mutations are known to be more severe than on other inbred strains [10,20].

The floxed mouse model and the approaches used in this study will provide a powerful tool for deciphering the physiological importance of *Atp7a* protein in a spatiotemporal context. As there are currently no effective treatments for Menkes disease, occipital horn syndrome or SMAX3, deciphering the phenotypic consequences tissue-specific *Atp7a* deletion may lead to new therapies for these disorders. Questions that we hope to address with this new animal model include the extent to which the neurological abnormalities in Menkes disease arise from a lack of copper delivery from the blood into the brain, versus a lack of ATP7A within the brain itself. Understanding such distinctions may have important implications for the development of membrane-permeable copper complexes able to carry copper ions across the blood brain barrier [21,22], or the design of viral

vectors that direct the expression of an *ATP7A* transgene in specific cell types of the brain in which a deficiency of *Atp7a* protein generates for the most severe neurological defects [20]. Addressing the requirement for *Atp7a* in motor neurons may shed light on the neuromuscular abnormality in patients with SMAX3. Of particular interest is whether SMAX3-like motor defects arise from copper toxicity in the motor neuron or a reduced copper delivery to cuproenzymes of the secretory pathway.

Notwithstanding the importance of ATP7A in these genetic disorders, numerous studies have also implicated ATP7A in a wide range of highly specialized processes beyond cellular copper homeostasis including glutamateric signaling and synaptogenesis in neurons [23,24], macrophage bactericidal activity [25], oxidation of low density lipoprotein particles [26], smooth muscle migration [27], Alzheimer's disease [28], and multidrug resistance in cancer cells [29,30]. Thus, the ability to selectively delete *Atp7a* in a tissue-specific manner may provide new insights into the broader roles of copper in normal physiology and disease states.

Materials and Methods

Animals and ethics

All animal husbandry and euthanasia procedures were performed in accordance with and under the approval of the Animal Care and Use Committee of the University of Missouri. All mice were on the C57BL6 strain background. Mice were maintained on 12 hour light-dark cycle and food and water provided *ad libitum*. Picolab diet 5053 (13 ppm Cu) was provided to mice at weaning and Picolab diet 5058 (17 ppm Cu) was provided during pregnancy and lactation (PMI International, St. Louis, MO, USA).

Generation of the *Atp7a* floxed mouse

Portions of the floxed mouse production were performed under contract by inGenious Targeting Laboratory, INC (Stonybrooke, NY). A 9.7 kb *PvuII* restriction fragment from a bacterial artificial chromosome library of C57BL6 mouse genomic DNA (clone RPC1-23-186F4) encompassing exons 8 to 13 of the *Atp7a* gene was subcloned into the pSP72 vector (Promega). A 62 bp single loxP cassette was inserted at a unique *KpnI* site located 123 bp upstream of the 5' splice boundary of exon 11. A neomycin cassette flanked by LoxP and FRT sites was excised from the plasmid pGK-gb2 loxP/FRT Neo (Gene Bridges GmbH, Germany) and inserted 313 bp downstream of the 3' splice exon 11 at unique *BamHI* site. The targeting vector was confirmed by sequencing. Ten micrograms of the targeting vector was linearized by *NotI* digestion and electroporated into C57BL/6 embryonic stem cells (Taconic, Hudson, NY), and single clones were selected for resistance to G418. Cell clones containing homologous insertion of long and short arms of the targeting vector were confirmed by southern blot and PCR analysis, and sequencing across LoxP sites and exons was used to verify fidelity of integration. Five independent correctly targeted clones were microinjected into Balb/c blastocysts and resulting chimeras with a high percentage black coat color were mated to wild-type C57BL6 mice to generate F1 offspring. Removal of the neomycin cassette via excision of flanking FRT sites was achieved by cross-breeding to FLP recombinase-expressing mice (strain B6.Cg-Tg(ACTFLPe)9205 Dym/J; Jackson Laboratory, Bar Harbor, ME). Floxed mice lacking the Neo cassette were identified by PCR analysis of tail genomic DNA and maintained on the C57BL6J background.

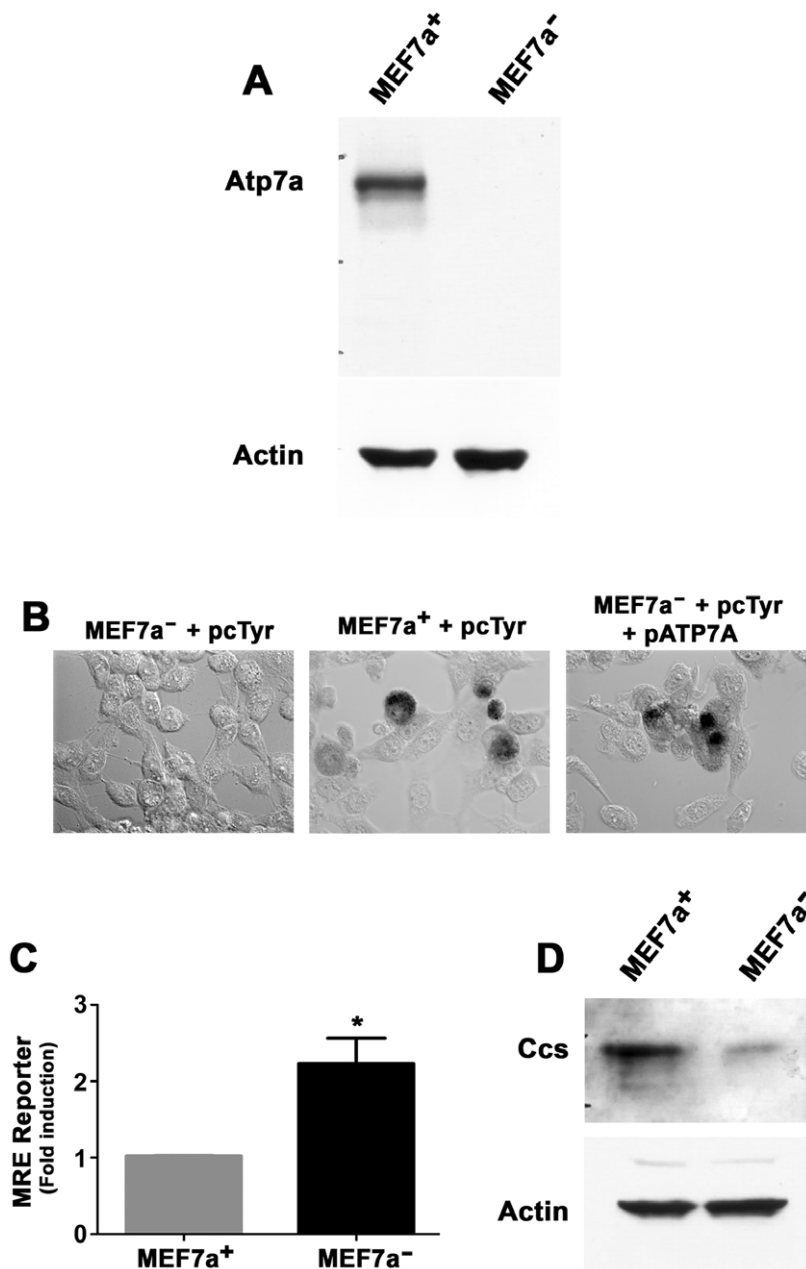


Figure 5. Characterization of MEF7a⁺ and MEF7a⁻ cells. A) Immunoblot analysis of Atp7a protein in MEF7a⁺ and MEF7a⁻ cells. Blots were probed with anti-Atp7a antibody (1:5000) followed by HRP-conjugated anti-rabbit antibody (1:5000). B) Defective copper delivery to tyrosinase MEF7a⁻ cells. MEF7a⁺ and MEF7a⁻ cells were transiently transfected with a plasmid encoding tyrosinase (pcTYR) alone, or in combination with a plasmid encoding ATP7A (pATP7A). Cells were then fixed in methanol and incubated with L-DOPA to allow the formation of the brown pigment, DOPACHrome. Note the absence of tyrosinase activity in MEF7a⁻ cells transfected with pcTYR alone (left), and complementation of this defect by co-transfection of pcTYR and pATP7A (right). C) MEF7a⁺ and MEF7a⁻ cells were transiently transfected with a Metal Responsive Element (MRE) reporter plasmid and a Renilla expression plasmid (pRL) as an internal control. After 24 hours, MRE luciferase activities of cell lysates were measured and normalized for Renilla luciferase activities. Experiments were repeated at least three times and values are presented as fold induction \pm SEM; * $p < 0.05$. D) Immunoblot analysis of Ccs protein in MEF7a⁺ and MEF7a⁻ cells. Blots were probed with anti-CCs antibody (1:500) followed by HRP-conjugated anti-rabbit antibody (1:5000). doi:10.1371/journal.pone.0043039.g005

Conditional knockout of *Atp7a*

To generate the global knockout, *Atp7a*^{fl/+} females were crossbred with *Cldn6*^{tm1(cre)Dkacw/J} mice (Jackson Laboratory). Tail snips from offspring were genotyped using PCR primers P1 (5'-GACAATACTACACTGACCATATTCA -3') and P2 (5'-GTCCACAGAACTATATGCCTGGG -3'). Detection of the Cre recombinase transgene was achieved using primers CreF

(5'-GATCGCTGCCAGGATATACG -3') and CreR (5'-AATCGC CATCTTCCAGCAG -3'). Timed pregnancy was established by confirmation of a copulation plug in female mice the morning after introduction to a breeding male, and this was designated as embryonic day E0.5 of pregnancy. At day E10.5, embryos were isolated from pregnant dams and the yolk sacs were

separated for genotyping as described above. Sex determination was performed as described previously [31].

Immunoblotting

Tissue samples and embryos were homogenized in ice-cold phosphate buffered saline (PBS) at pH 7.4, and protein lysates were prepared by sonicating cell pellets in lysis buffer containing 2.5 mM Tris-HCl (pH 7.4), 2% sodium dodecyl sulfate, 1% Triton X-100, 1 mM EDTA and CompleteTM protease inhibitor (Roche Molecular Biochemicals, Indianapolis, IN). Protein lysates were fractionated by 7.5% sodium dodecyl sulfate-polyacrylamide gel electrophoresis and transferred onto nitrocellulose membranes. The membranes were blocked with 1% casein solution and incubated in blocking buffer at 4°C overnight with a rabbit anti-Atp7a antibody, described previously [32], raised against the terminal 20 amino acids (1:5000 dilution) or mouse β -actin antibody (1:5000) (abcam, Cambridge, MA). Horseradish peroxidase conjugated goat anti-rabbit IgG or goat anti-mouse IgG (1:5000) were used as secondary antibodies, and blots were developed using the SuperSignal West Pico Substrate according to the manufacturer's instructions (Pierce, Rockford, IL).

Isolation and Culture of Mouse Embryonic Cells

Hemizygous male floxed embryos (*Atp7a*^{fl/y}) were dissected from the decidua at embryonic day 13.5 and all tissues remaining after removal of the head and internal organs were minced with scissors and then incubated in 0.25% trypsin at 37°C for 15 minutes to facilitate dispersal into a single cell suspension. The cells were then cultured in complete medium (Dulbecco's modified Eagle's medium supplemented with 10% fetal bovine serum, 2 mM glutamine and 100 units/ml penicillin and streptomycin). After 3 weeks of culture, the cells were passaged onto 100 mm dishes and transfected with the pSV3-neo plasmid carrying SV40 large T antigen gene using the LipoD293 transfection reagent (SigmaGen, Rockville, MD), and selected for resistance to neomycin. Single colonies were then expanded to generate multiple immortalized MEF7a⁺ cell lines. To generate an isogenic cell line lacking Atp7a

protein expression (MEF7a⁻ cells), the *Atp7a* gene was deleted by transient transfection of one MEF7a⁺ cell clone with a plasmid carrying the Cre recombinase gene fused to GFP (pCAG-Cre: GFP; Addgene, Cambridge, MA). Cells enriched for GFP expression were sorted into 96 well trays by fluorescence activated cell sorting, and single clones were expanded. Deletion of the *Atp7a* gene was confirmed by PCR genotyping.

Luciferase Reporter Assay

MEF7a⁺ and MEF7a⁻ cells were seeded in 96-well plates and transiently transfected with 35 ng of the MRE-luciferase reporter [33], and 3.5 ng of Renilla luciferase plasmid (pRL) using LipoD293 transfection reagent (SigmaGen Laboratories). After a 24-hour incubation in complete medium, the firefly luciferase activity and Renilla luciferase activity were assayed by luminometer (Veritas) using the Dual-Glo luciferase assay system (Promega, Madison, WI). The relative light units (RLU) were calculated by dividing firefly luciferase activity by Renilla luciferase activity. Fold induction was calculated as mean RLU produced by MEF7a⁻ cells divided by mean RLU produced by MEF7a⁺ cells.

In Situ Tyrosinase Activity Assay

In situ tyrosinase activity was conducted in MEF cells as previously described by detecting the formation of brown DOPA-chrome from the oxidation of colorless L-DOPA [14].

Acknowledgments

We thank all members of our laboratories for their support and helpful comments.

Author Contributions

Conceived and designed the experiments: YW JDG MJP. Performed the experiments: YW SZ. Analyzed the data: YW SZ MJP. Contributed reagents/materials/analysis tools: GAW. Wrote the paper: YW SZ JDG MJP.

References

- Kaler SG (2011) ATP7A-related copper transport diseases-emerging concepts and future trends. *Nature reviews Neurology* 7: 15–29.
- Kambe T, Weaver BP, Andrews GK (2008) The genetics of essential metal homeostasis during development. *Genesis* 46: 214–228.
- Petris MJ, Mercer JF, Culvenor JG, Lockhart P, Gleeson PA, et al. (1996) Ligand-regulated transport of the Menkes copper P-type ATPase efflux pump from the Golgi apparatus to the plasma membrane: a novel mechanism of regulated trafficking. *The EMBO journal* 15: 6084–6095.
- Yamaguchi Y, Heiny ME, Suzuki M, Gitlin JD (1996) Biochemical characterization and intracellular localization of the Menkes disease protein. *Proceedings of the National Academy of Sciences of the United States of America* 93: 14030–14035.
- Kaler SG, Gallo LK, Proud VK, Percy AK, Mark Y, et al. (1994) Occipital horn syndrome and a mild Menkes phenotype associated with splice site mutations at the MNK locus. *Nat Genet* 8: 195–202.
- Volpintesta EJ (1974) Menkes kinky hair syndrome in a black infant. *American journal of diseases of children* 128: 244–246.
- Kennerson ML, Nicholson GA, Kaler SG, Kowalski B, Mercer JF, et al. (2010) Missense mutations in the copper transporter gene ATP7A cause X-linked distal hereditary motor neuropathy. *American journal of human genetics* 86: 343–352.
- Levinson B, Packman S, Gitschier J (1997) Deletion of the promoter region in the *Atp7a* gene of the mottled dappled mouse. *Nature Genetics* 16: 224–225.
- Mercer JF, Grimes A, Ambrosini L, Lockhart P, Paynter JA, et al. (1994) Mutations in the murine homologue of the Menkes gene in dappled and blotchy mice. *Nature Genetics* 6: 374–378.
- Mototani Y, Miyoshi I, Okamura T, Moriya T, Meng Y, et al. (2006) Phenotypic and genetic characterization of the *Atp7a*(Mo-Tohm) mottled mouse: a new murine model of Menkes disease. *Genomics* 87: 191–199.
- Mercer JF (1998) Menkes syndrome and animal models. *The American journal of clinical nutrition* 67: 1022S–1028S.
- Lyon MF (1961) Gene action in the X-chromosome of the mouse (*Mus musculus* L.). *Nature* 190: 372–373.
- Hunt DM (1974) Primary defect in copper transport underlies mottled mutants in the mouse. *Nature* 249: 852–854.
- Petris MJ, Strausak D, Mercer JF (2000) The Menkes copper transporter is required for the activation of tyrosinase. *Hum Mol Genet* 9: 2845–2851.
- Caruano-Yzermans AL, Bartnikas TB, Gitlin JD (2006) Mechanisms of the copper-dependent turnover of the copper chaperone for superoxide dismutase. *J Biol Chem* 281: 13581–13587.
- Prohaska JR, Broderius M, Brokate B (2003) Metallochaperone for Cu, Zn-superoxide dismutase (CCS) protein but not mRNA is higher in organs from copper-deficient mice and rats. *Arch Biochem Biophys* 417: 227–234.
- Czyzyk TA, Ning Y, Hsu MS, Peng B, Mains RE, et al. (2005) Deletion of peptide amidation enzymatic activity leads to edema and embryonic lethality in the mouse. *Dev Biol* 287: 301–313.
- Maki JM, Rasanen J, Tikkanen H, Sormunen R, Makikallio K, et al. (2002) Inactivation of the lysyl oxidase gene *Lox* leads to aortic aneurysms, cardiovascular dysfunction, and perinatal death in mice. *Circulation* 106: 2503–2509.
- Thomas SA, Matsumoto AM, Palmiter RD (1995) Noradrenaline is essential for mouse fetal development. *Nature* 374: 643–646.
- Donsante A, Yi L, Zerfas PM, Brinster LR, Sullivan P, et al. (2011) ATP7A Gene Addition to the Choroid Plexus Results in Long-term Rescue of the Lethal Copper Transport Defect in a Menkes Disease Mouse Model. *Molecular therapy: the journal of the American Society of Gene Therapy*.
- Green MA, Klippenstein DL, Tennison JR (1988) Copper(II) bis(thiosemicarbazone) complexes as potential tracers for evaluation of cerebral and myocardial blood flow with PET. *J Nucl Med* 29: 1549–1557.
- Crouch PJ, Hung LW, Adlard PA, Cortes M, Lal V, et al. (2009) Increasing Cu bioavailability inhibits Abeta oligomers and tau phosphorylation. *Proc Natl Acad Sci U S A* 106: 381–386.
- Schlieff ML, Craig AM, Gitlin JD (2005) NMDA receptor activation mediates copper homeostasis in hippocampal neurons. *The Journal of neuroscience: the official journal of the Society for Neuroscience* 25: 239–246.

24. El Meskini R, Crabtree KL, Cline LB, Mains RE, Eipper BA, et al. (2007) ATP7A (Menkes protein) functions in axonal targeting and synaptogenesis. *Mol Cell Neurosci* 34: 409–421.
25. White C, Lee J, Kambe T, Fritsche K, Petris MJ (2009) A role for the ATP7A copper-transporting ATPase in macrophage bactericidal activity. *The Journal of biological chemistry* 284: 33949–33956.
26. Qin Z, Konanah ES, Neltner B, Nemenoff RA, Hui DY, et al. (2010) Participation of ATP7A in macrophage mediated oxidation of LDL. *Journal of lipid research* 51: 1471–1477.
27. Ashino T, Sudhakar V, Urao N, Oshikawa J, Chen GF, et al. (2010) Unexpected role of the copper transporter ATP7A in PDGF-induced vascular smooth muscle cell migration. *Circulation research* 107: 787–799.
28. Zheng Z, White C, Lee J, Peterson TS, Bush AI, et al. (2010) Altered microglial copper homeostasis in a mouse model of Alzheimer's disease. *J Neurochem* 114: 1630–1638.
29. Samimi G, Safaei R, Katano K, Holzer AK, Rochdi M, et al. (2004) Increased expression of the copper efflux transporter ATP7A mediates resistance to cisplatin, carboplatin, and oxaliplatin in ovarian cancer cells. *Clin Cancer Res* 10: 4661–4669.
30. Owatari S, Akune S, Komatsu M, Ikeda R, Firth SD, et al. (2007) Copper-transporting P-type ATPase, ATP7A, confers multidrug resistance and its expression is related to resistance to SN-38 in clinical colon cancer. *Cancer Res* 67: 4860–4868.
31. Clapcote SJ, Roder JC (2005) Simplex PCR assay for sex determination in mice. *Biotechniques* 38: 702, 704, 706.
32. Zheng Z, White C, Lee J, Peterson TS, Bush AI, et al. (2010) Altered microglial copper homeostasis in a mouse model of Alzheimer's disease. *Journal of Neurochemistry* 114: 1630–1638.
33. van den Berghe PV, Folmer DE, Malingre HE, van Beurden E, Klomp AE, et al. (2007) Human copper transporter 2 is localized in late endosomes and lysosomes and facilitates cellular copper uptake. *Biochem J* 407: 49–59.